NRC Research Press

ARTICLE

Stand age versus tree diameter as a driver of forest carbon inventory simulations in the northeastern U.S.

Wu Ma, Christopher W. Woodall, Grant M. Domke, Anthony W. D'Amato, and Brian F. Walters

Abstract: Estimating the current status and future trends of carbon (C) stocks and stock changes in forests of the northeastern United States is desired by policy makers and managers as these forests can mitigate climate change through sequestration of atmospheric carbon dioxide (CO_2). We developed C flux matrix models using tree and stand variables by tree diameter class and stand age class to compare size-structured models with age-structured models in their capacity to predict forest C dynamics that are central to policy decisions. The primary control variables for the C flux matrix models (diameter at breast height, stand basal area, stem density, and stand age) were all statistically significant at the $\alpha \leq 0.05$ level. Through comparing the simulation results and root mean square error of C flux matrix models by tree diameter class and stand age class, we found that tree diameter class more accurately predicted C stock change status across the broad compositional and structural conditions in the spatial and temporal domain. An uncertainty analysis revealed that predictions of aboveground C and soil C would be distinctively different whether using tree diameter class or stand age class with high certainty. Overall, this work may enable better integration of forest inventory data and remotely sensed data for the purpose of strategic-scale forest C dynamic simulations.

Key words: forest C dynamic, matrix models, diameter class, age class, uncertainty.

Résumé : Les décideurs politiques et les aménagistes souhaitent avoir une estimation de l'état actuel et des tendances futures des stocks de carbone (C) ainsi que des variations des stocks dans les forêts du nord-est des États-Unis étant donné que ces forêts peuvent atténuer le changement climatique en séquestrant le CO_2 atmosphérique. Nous avons conçu des modèles de matrice du flux de C à l'aide de variables de l'arbre et du peuplement fondés soit sur la classe de diamètre des arbres, soit sur la classe d'âge des peuplements dans le but de comparer les modèles structurés par la taille et ceux structurés par l'âge quant à leur capacité à prédire la dynamique du C forestier qui est au cœur des décisions stratégiques. Les variables de contrôle primaires dans les modèles de matrice du flux de C (le diamètre à hauteur de poitrine, la surface terrière du peuplement, la densité des tiges et l'âge du peuplement) étaient toutes statistiquement significatives ($\alpha \leq 0{,}05$). En comparant les résultats de la simulation et l'erreur quadratique moyenne des modèles de matrice du flux de C fondés sur la classe de diamètre des arbres et ceux fondés sur la classe d'âge des peuplements, nous avons trouvé que la classe de diamètre des arbres prédisait avec plus d'exactitude la variation de l'état des stocks de C pour l'ensemble des grandes conditions de composition et de structure dans les domaines spatial et temporel. Une analyse d'incertitude a révélé que les prédictions du C aérien et du C dans le sol seraient avec une grande certitude nettement différentes selon qu'on utilise la classe de diamètre des arbres ou la classe d'âge des peuplements. Dans l'ensemble cette étude peut aider à mieux intégrer les données d'inventaire forestier et les données de télédétection pour simuler la dynamique du C forestier à une échelle stratégique. [Traduit par la Rédaction]

Mots-clés : dynamique du carbone forestier, modèles de matrice, classe de diamètre, classe d'âge, incertitude.

Introduction

As forests are the largest terrestrial carbon (C) sink (Pan et al. 2011*a*) on Earth, nations have developed greenhouse gas (GHG) emission reduction targets inclusive of the land sector, with forest lands being identified as a relatively cost-effective means to reduce C emissions. Forest net C sequestration can mitigate the effects of C emissions to the atmosphere; therefore, the monitoring of forest C stocks is critical to understanding the drivers of C stock change across terrestrial ecosystems over time. Forest growth, regeneration, and mortality are three main components of forest population and related carbon dynamics (Swaine et al. 1987; Felfili 1995; Huth and Ditzer 2001; Rice et al. 2004). Unfortunately, there is much uncertainty associated with estimates of forest C stock changes due to the combined effects of variability in tree growth, recruitment, and mortality rates (Vieira et al. 2004). Examinations of drivers of C dynamics in regions occupied by a diversity of tree species and stand structural combinations such as the northeastern United States (US) may be useful to informing science and policy at multiple scales (e.g., regional to international) that seek to reduce net C emissions (Evans and Perschel 2009). Furthermore, studies characterizing forest ecosystem dynamics may assist with forest management activities. The simulation of forest C dynamics across temporal scales in this region, even over short time frames (e.g., 5–30 years), remains a substantial knowledge gap critical to C emission mitigation strategies and annual reporting requirements (e.g., United Nations Framework Convention on Climate Change, UNFCCC);

Received 20 January 2018. Accepted 11 July 2018.

W. Ma and A.W. D'Amato. Rubenstein School of Environment and Natural Resources, University of Vermont, Burlington, VT 05405, USA.
C.W. Woodall. U.S. Department of Agriculture, Forest Service, Northern Research Station, Durham, NH 03824-0640, USA.
G.M. Domke and B.F. Walters. U.S. Department of Agriculture, Forest Service, Northern Research Station, St. Paul, MN 55108, USA.
Corresponding author: Wu Ma (email: wu.ma@uvm.edu).

hence, there is great need to improve the prediction of forest C dynamics.

The distribution of forest developmental stages, as reflected in stand age and tree size distributions, across a region strongly affects potential C accumulation at landscape and regional scales (i.e., the population; Rhemtulla et al. 2009). Correspondingly, empirical models with tree diameter class and stand age class, as well as process-based models, have been developed to simulate forest C dynamics. For example, landscape-scale models of forest succession, disturbance, and C dynamics (e.g., LANDIS-II) have been used to evaluate the effects of a changing climate on total forest C, tree species composition, and wildfire dynamics (e.g., Loudermilk et al. 2013). In the northeastern US, the Forest Vegetation Simulator (FVS) was used to conduct a comparison of C stock estimates for regional carbon estimation (MacLean et al. 2014) and dynamics of late-successional and old-growth forest C (Gunn et al. 2014). Matrix models use transition matrices to estimate the dynamics of ecological populations (e.g., Caswell 2001; Fieberg and Ellner 2001; Liang and Picard 2013). Dating back to the 1940s (Leslie 1945; Lewis 1977), matrix models have been widely employed to study forest ecosystem dynamics due to their accuracy and robustness in depicting forest populations. Today, techniques of deterministic matrix models have been extended to environmental stochastic matrix models and climate-sensitive models to account for natural disturbances and climate change (see Liang and Picard (2013) and references therein).

Matrix models of varying degrees of complexity have also been applied to estimate forest population dynamics and associated forest C dynamics, with stand age or species-specific diameter classes often used as predictor variables (e.g., Solomon et al. 1987, 1995, 2000; Gove and Ducey 2014; Liang and Zhou 2014; Wear and Coulston 2015; Ma et al. 2016; Ma and Zhou 2018). For example, Gove and Ducey (2014) employed a matrix model to predict spruce–fir forest dynamics using tree diameter class. Liang and Zhou (2014) used a geospatial matrix model to estimate the amount of carbon dioxide (CO_2) equivalent sequestered by live trees using tree diameter class. Wear and Coulston (2015) developed a matrix model to estimate net sequestration of atmospheric C on forest land using stand age class. Ma et al. (2016) built an integrated matrix model with tree diameter class to synchronously couple forest dynamics, mean fire interval, population density, and future climate scenarios for US Central Hardwood Region forests. Ma and Zhou (2018) quantified how various harvesting intensities would influence C stock under climate and fire uncertainty from 2010 to 2100 using tree diameter class. Despite these advances over the past few years, simulation techniques of forest C inventories that align with the Intergovernmental Panel on Climate Change's (IPCC) Good Practice Guidance (IPCC 2006; e.g., all forest C pools and land uses from 1990 to the present) and incorporate annual forest inventory data over large scales have remained elusive for the US (Woodall et al. 2015).

The goal of this study was to compare size-structured models with age-structured models in their capacity to estimate forest C stock dynamics, using C flux matrix models by tree diameter class and stand age class over 5 years with comparison by C pools. Total forest C includes a variety of non-overlapping C pools considered in various reporting instruments: aboveground live tree, belowground live tree, aboveground dead tree, belowground dead tree, aboveground live sapling, belowground live sapling, aboveground understory, belowground understory, litter, soil, standing dead, and downed dead in addition to the five IPCC pools (aboveground biomass, belowground biomass, dead, litter, and soil; Woodall et al. 2015). The objectives included developing C flux matrix models by species-specific diameter class for the Northern Forest region of the northeastern US to identify the relative influences of forest growth, regeneration, and mortality. Based on these results, C flux matrix models with stand age class were developed to explore the effects of age class distributions. Finally, comparisons of predictions of forest C stocks and stock changes with stand age class versus tree diameter class were made to meet the overall goal of refined understanding of regional forest C dynamics.

Data and methods

Forest data

The Northern Forest region of the northeastern US covers the states of Maine, New Hampshire, New York, and Vermont and contains a wide range of climatic conditions, ecoregions, stand conditions, and species composition (Fig. 1). We included 6472 re-measured permanent ground plots from the USDA Forest Service's Forest Inventory and Analysis (FIA) database (USDA Forest Service 2014). Each permanent ground plot comprises four smaller fixed-radius (7.32 m) subplots spaced 36.6 m apart in a triangular arrangement with one subplot in the center (USDA Forest Service 2015). From these, 5178 permanent ground plots with at least one forested condition (80% of total 6472 plots) were used for model calibration following three criteria. First, plots had to be re-measured (5–7 years, previous measurement in 2004–2010 with same plots re-measured once in 2010–2015, which results in an inconsistent time gap between plot measurements). Second, plots had to have at least one live tree at the time of both measurements. Finally, plots were located in forests without any evidence of silvicultural treatments or any other forms of anthropogenic disturbance (e.g., cutting and artificial regeneration) as defined and classified in the FIA program. For validation purposes, we randomly selected 1294 permanent ground plots (20% of total 6472 plots) throughout the region to test model accuracy (Fig. 1).

For each sample plot, plot-level attributes included fuzzed coordinates (a technique applied to FIA plot coordinates to follow privacy laws while maintaining a good correlation between the plot data and map-based coordinates, USDA Forest Service 2015), site productivity, stand density, basal area, slope, elevation, and 12 previously defined C pools and five IPCC pools (Supplementary Table S1[1]). Tree-level data, including species, diameter, and status (recruitment, live, or dead), were also collected on each plot. The research area is largely dominated by six major species: red maple (*Acer rubrum* L.), balsam fir (*Abies balsamea* (L.) Mill.), sugar maple (*Acer saccharum* Marsh.), eastern white pine (*Pinus strobus* L.), eastern hemlock (*Tsuga canadensis* (L.) Carrière), and red spruce (*Picea rubens* Sarg.) (Supplementary Table S2[1]). Red maple had the highest basal area of all of the species (13.51%), followed by balsam fir (11.02%), sugar maple (9.87%), eastern white pine (7.70%), eastern hemlock (7.30%), and red spruce (6.76%) (Supplementary Table S2[1]). For simplicity and computational efficiency, we classified all tree species into six species groups from the FIA program: maple–beech–birch, spruce–fir, white–red–jack pine, aspen–birch, oak–hickory, and other species (Supplementary Table S2[1]). Within each species group, trees were further categorized into 17 diameter at breast height classes of 5 cm increments, except for the first class (2.54–7 cm) and the last (82 cm and above). As observed in Supplementary Table S4[1], negative diameter growth values accounted for less than 3% of the total population and were mainly due to measurement errors and shrinkage. These negative values were also used for fitting the diameter growth model with the rest of data as the same contribution of measurement errors could also be observed on the high-growth end of the diameter growth distribution. In addition, we constructed 34 age classes of 5-year age increases for all FIA plots by C density from ages 1–5,

[1]Supplementary material is available with the article through the journal Web site at http://nrcresearchpress.com/doi/suppl/10.1139/cjfr-2018-0019.

Fig. 1. Approximate geographic distribution of the calibration (dots) and validation (+) plots in the Northern Forest region of the northeastern US. [Colour version online.]

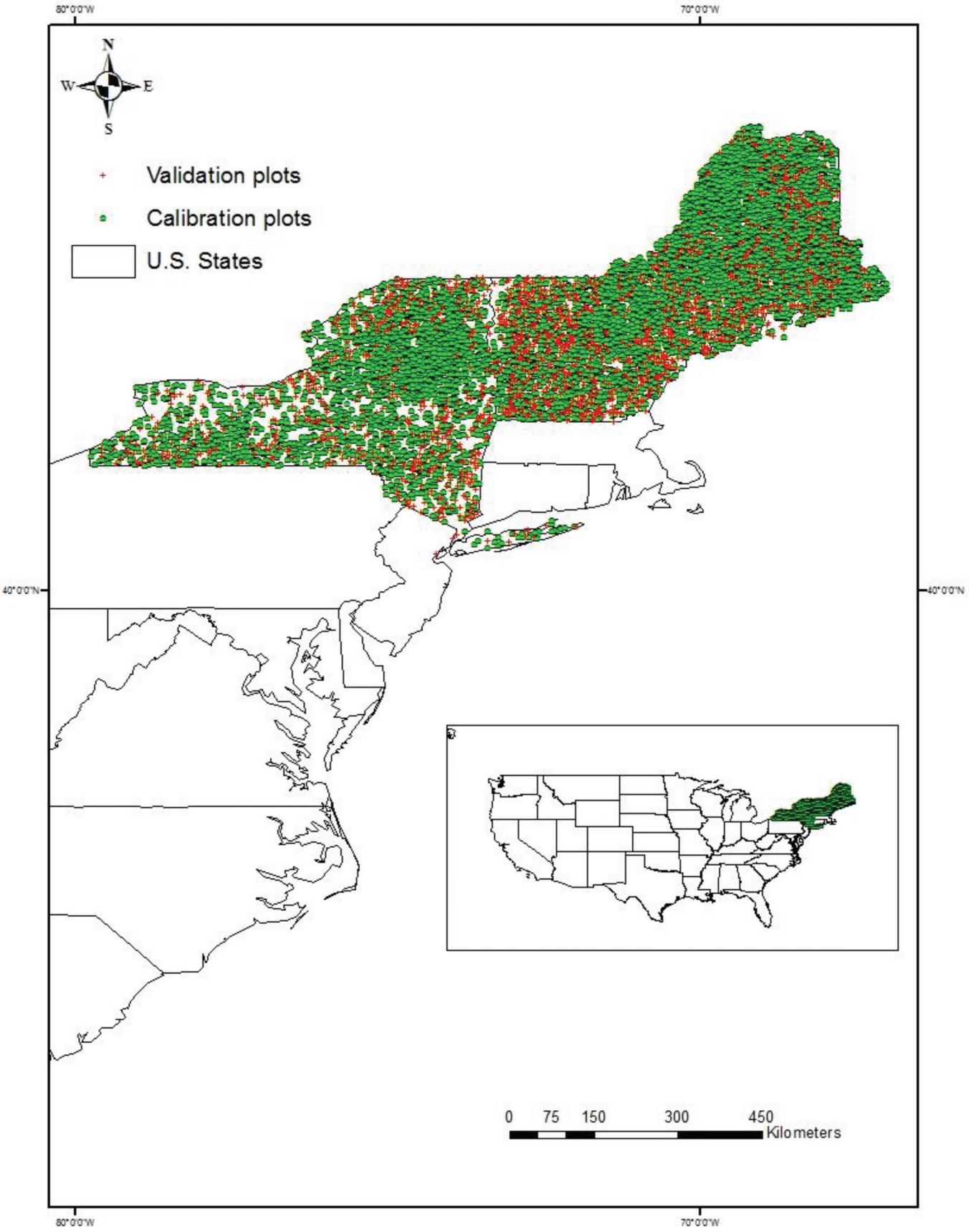

Table 1. Definitions and units of variables used in the study.

Variable	Unit	Definition or explanation
B	$m^2 \cdot ha^{-1}$	Total stand basal area
C		Site productivity class
D	cm	Diameter at breast height
g	$cm \cdot year^{-1}$	Annual diameter growth
E	km	Plot elevation
S	degrees	Plot slope
H_d		Tree size diversity in Shannon's index
H_s		Tree species diversity in Shannon's index
T	°C	Mean annual temperature
P	100 mm	Mean annual precipitation
m	$year^{-1}$	Annual tree mortality
N	$trees \cdot ha^{-1}$	Number of trees per hectare
R	$trees \cdot ha^{-1} \cdot year^{-1}$	Recruitment, the number of trees per hectare growing into the smallest diameter class (2.54–7 cm) in a year
AGL	$Mg \cdot ha^{-1}$	Carbon in live tree aboveground
BGL	$Mg \cdot ha^{-1}$	Carbon in live tree belowground
AGD	$Mg \cdot ha^{-1}$	Carbon in dead tree aboveground
BGD	$Mg \cdot ha^{-1}$	Carbon in dead tree belowground
AGLS	$Mg \cdot ha^{-1}$	Carbon in live sapling aboveground
BGLS	$Mg \cdot ha^{-1}$	Carbon in live sapling belowground
AGU	$Mg \cdot ha^{-1}$	Carbon in understory aboveground
BGU	$Mg \cdot ha^{-1}$	Carbon in understory belowground
Litter	$Mg \cdot ha^{-1}$	Carbon in litter
Soil	$Mg \cdot ha^{-1}$	Carbon in organic soil
SD	$Mg \cdot ha^{-1}$	Carbon in standing dead
DD	$Mg \cdot ha^{-1}$	Carbon in downed dead
I_AGB	$Mg \cdot ha^{-1}$	Carbon in the IPCC biomass aboveground
I_BGB	$Mg \cdot ha^{-1}$	Carbon in the IPCC biomass belowground
I_Dead	$Mg \cdot ha^{-1}$	Carbon in the IPCC dead wood
I_Litter	$Mg \cdot ha^{-1}$	Carbon in the IPCC litter
I_Soil	$Mg \cdot ha^{-1}$	Carbon in the IPCC organic soil

6–10, 11–15, …, to 170+ years. The FIA stand age was estimated from a sample of tree ages. Note that many of these plots are likely in multi-aged stands for which ascribing a stand age is not appropriate and therefore age classifications largely serve as a relative index of developmental stage.

C flux matrix models

We used matrix models to evaluate forest C dynamics in this study. Carbon flux matrix models were constructed as follows:

$$\boldsymbol{y}_{t+1} = \mathbf{G}_t \cdot \boldsymbol{y}_t + \boldsymbol{R}_t + \varepsilon \quad (1)$$

in which $\boldsymbol{y}_t$ is a column vector representing the number of live trees per diameter class at time t; $\mathbf{G}_t$ is the growth matrix describing the transition of trees between size classes as well as mortality; $\boldsymbol{R}_t$ is a regeneration vector; and ε is an error term.

A variety of explanatory variables for six species groups (Supplementary Table S2[1]) were examined in this study (Table 1). Diameter and its square (D and D^2, respectively) were used in the individual-tree models (diameter growth, mortality) to capture the nonlinear effects of diameter. Stand age and its square (A and A^2, respectively) were used in the C move models to explore the effects of age. The stand density of that species and its square (N and N^2, respectively), representing the size of the seed bank (Peterson et al. 2014), were only used in the stand-level recruitment model. Many existing matrix models used total basal area (B) and site productivity (C) as key predictors because of their significant effects on forest dynamics (Namaalwa et al. 2005; Boltz and Carter 2006). Physiographic variables elevation (E) and slope (S) were used to control for site productivity (Lennon et al. 2002). In addition, stand diversity metrics of structural and species diversity were included to explicitly account for the effects of diversity on forest dynamics (i.e., positive relationship between plant diversity and net ecosystem productivity; Liang et al. 2007).

Table 2. Summary statistics of 12 carbon pools and five IPCC carbon pools ($Mg \cdot ha^{-1}$) across the study region.[a]

Statistic	Mean	SD	Maximum	Minimum
Current (2010–2015)				
AGL	59.45	66.10	3357.42	0.25
BGL	12.09	13.12	649.38	0.06
AGD	1.89	4.63	134.14	0.00
BGD	0.55	1.22	25.99	0.00
AGLS	6.25	9.48	284.99	0.00
BGLS	1.43	2.12	61.08	0.00
AGU	1.54	0.22	5.49	1.06
BGU	0.17	0.02	0.61	0.12
Litter	15.62	3.73	94.82	4.27
Soil	138.76	20.07	347.37	91.97
SD	6.08	1.53	24.30	0.00
DD	5.19	2.33	51.37	0.16
I_AGB	66.08	66.16	3357.42	0.84
I_BGB	13.56	13.11	649.38	0.15
I_Dead	3.69	5.85	160.69	0.00
I_Litter	3.81	1.05	23.71	0.01
I_Soil	39.27	7.62	86.84	0.75
Previous (2004–2010)				
AGL	56.14	61.22	3057.36	0.00
BGL	11.42	12.26	585.25	0.00
AGD	1.80	4.51	134.22	0.00
BGD	0.51	1.06	24.37	0.00
AGLS	6.11	9.37	274.21	0.00
BGLS	1.39	2.11	58.13	0.00
AGU	1.48	0.13	5.08	0.96
BGU	0.15	0.01	0.28	0.08
Litter	14.86	5.28	94.32	4.06
Soil	128.34	19.43	320.11	89.57
SD	6.00	1.47	22.72	0.00
DD	5.05	2.19	45.76	0.11
I_AGB	63.31	61.27	3057.37	0.01
I_BGB	13.01	12.27	585.25	0.00
I_Dead	3.61	5.85	162.30	0.00
I_Litter	3.62	1.38	23.71	0.04
I_Soil	36.95	7.06	80.03	0.52

Note: SD, standard deviation.

[a]Study region: the Northern Forest region of the northeastern US covering the states of Maine, New Hampshire, New York, and Vermont.

Matrix model structure for diameter class

$\mathbf{G}_t$ and $\mathbf{G}_{it}$ are matrices used to model dynamics of forest population, where

$$\mathbf{G}_t = \begin{bmatrix} \mathbf{G}_{1t} & & & \\ & \mathbf{G}_{2t} & & \\ & & \ddots & \\ & & & \mathbf{G}_{i,t} \end{bmatrix}$$

$$\mathbf{G}_{it} = \begin{bmatrix} a_{i1,t} & & & & \\ b_{i1,t} & a_{i2,t} & & & \\ & \ddots & \ddots & & \\ & & b_{i,j-2,t} & a_{i,j-1,t} & \\ & & & b_{i,j-1,t} & a_{i,j,t} \end{bmatrix} \quad (2)$$

in which a_{ijt} represents the probability that a tree of species i and diameter class j stays alive in the same diameter class between t and $t + 1$; and b_{ijt}, the upgrowth transition rate that a tree of species i and diameter class j stays alive and grows into diameter

Table 3. Estimated parameters of the diameter growth models.

Diameter growth models	R^2
Maple–beech–birch	
$1.357^{***} + 0.034D^{**} - 0.002D^{2***} - 0.036B^{**} - 0.021C^{*} - 0.126H_d^{**} - 0.039H_s^{**} - 0.052E^{*} - 0.001S^{**}$	0.76
Spruce–fir	
$1.523^{**} + 0.037D^{***} - 0.001D^{2**} - 0.037B^{**} - 0.029C^{*} - 0.012H_d^{*} + 0.123H_s^{**} - 0.046E^{*} + 0.002S^{*}$	0.68
White–red–jack pine	
$1.342^{**} + 0.038D^{**} - 0.0002D^{2***} - 0.034B^{***} + 0.029C^{*} - 0.037H_d^{*} - 0.016H_s^{*} - 0.348E^{*} - 0.002S^{**}$	0.63
Aspen–birch	
$1.694^{**} + 0.023D^{**} - 0.001D^{2**} - 0.038B^{**} + 0.003C^{*} + 0.062H_d^{*} - 0.592H_s^{*} - 0.157E^{**} - 0.003S^{**}$	0.61
Oak–hickory	
$1.567^{**} + 0.027D^{**} - 0.0001D^{2*} - 0.086B^{**} - 0.097C^{**} - 0.089H_d^{**} + 0.118H_s^{**} - 0.106E^{*} - 0.0001S^{*}$	0.56
Other species	
$1.468^{**} + 0.003D^{*} - 0.002D^{2**} - 0.037B^{**} - 0.043C^{*} - 0.026H_d^{*} - 0.512H_s^{***} + 0.004E - 0.003S^{**}$	0.53

Note: Significance levels: *, <0.05; **, <0.01; ***, <0.001.

Table 4. Estimated parameters of the mortality models.

Mortality models	R^2
Maple–beech–birch	
$0.652^{*} + 0.008D^{**} - 0.0002D^{2**} + 0.076B^{**} + 0.026C^{*} - 0.813H_d^{**} - 0.426H_s^{**} - 0.067E^{*} - 0.0001S$	0.25
Spruce–fir	
$0.756^{*} + 0.042D^{**} - 0.001D^{2***} + 0.037B^{**} - 0.026C^{**} - 0.932H_d^{*} + 0.298H_s^{**} - 0.081E^{**} + 0.002S^{*}$	0.21
White–red–jack pine	
$0.684^{*} + 0.007D^{**} - 0.0002D^{2**} + 0.059B^{***} - 0.003C^{*} - 1.642H_d^{**} + 0.091H_s^{*} - 0.126E^{*} - 0.003S^{**}$	0.19
Aspen–birch	
$0.526^{*} + 0.033D^{***} - 0.001D^{2***} + 0.064B^{**} + 0.062C^{**} - 0.624H_d^{**} - 0.136H_s^{*} - 0.033E - 0.001S^{*}$	0.16
Oak–hickory	
$0.861^{*} + 0.006D^{***} - 0.0002D^{2***} + 0.079B^{***} - 0.034C - 0.956H_d^{**} - 0.028H_s^{*} - 0.086E^{*} - 0.002S$	0.17
Other species	
$0.723^{*} + 0.002D^{***} - 0.001D^{2***} + 0.096B^{***} - 0.004C - 0.037H_d^{**} - 0.086H_s^{*} - 0.061E - 0.001S^{*}$	0.20

Note: Significance levels: *, <0.05; **, <0.01; ***, <0.001.

Table 5. Estimated parameters of the recruitment models.

Recruitment models	R^2
Maple–beech–birch	
$-1.634^{**} + 0.267N^{***} - 0.164N^{2***} - 2.586B^{**} + 1.624C^{**} + 1.296H_d^{*} + 1.364H_s^{**} + 1.526E - 0.951S^{**}$	0.34
Spruce–fir	
$-1.352^{*} + 0.347N^{***} - 0.084N^{2**} - 2.237B^{***} - 2.259C^{*} + 0.654H_d^{**} + 1.516H_s^{*} - 1.062E^{*} - 0.632S^{*}$	0.38
White–red–jack pine	
$-1.956^{*} + 0.352N^{**} - 0.321N^{2**} - 1.852B^{***} - 0.467C^{*} + 0.523H_d^{**} + 2.132H_s^{**} - 0.523E^{*} - 0.628S$	0.29
Aspen–birch	
$-1.634^{*} + 0.564N^{***} - 0.378N^{2***} - 2.869B^{***} - 1.895C^{*} - 0.864H_d^{*} + 1.826H_s^{**} - 0.894E^{**} + 0.846S^{*}$	0.25
Oak–hickory	
$-1.812^{*} + 0.642N^{***} - 0.385N^{2***} - 2.298B^{***} - 0.589C^{**} + 0.385H_d^{*} + 2.867H_s^{*} - 1.214E^{*} - 0.594S$	0.27
Other species	
$-1.852 + 0.467N^{***} - 0.467N^{2***} - 2.267B^{***} - 0.895C^{*} + 0.674H_d^{*} + 2.963H_s^{*} - 0.348E^{**} - 0.964S^{*}$	0.31

Note: Significance levels: *, <0.05; **, <0.01; ***, <0.001.

class $j + 1$ between t and $t + 1$, is estimated as the annual tree diameter growth (g_{ijt}) divided by the width of the diameter class, assuming that g_{ijt} stays constant within each diameter class. Because b_{ijt} represents a probability, it must be lower than 1; hence, $g_{ijt} \leq$ the width of the diameter class. a_{ijt} and b_{ijt} are related by

$$a_{ijt} = 1 - b_{ijt} - m_{ijt} \quad (3)$$

where m_{ijt} is the probability of tree mortality between t and $t + 1$.

$\boldsymbol{R}$ is a state- and time-dependent recruitment vector representing the number of trees naturally recruited in the smallest diameter class of each species, between t and $t + 1$:

$$\boldsymbol{R}_t = \begin{bmatrix} \boldsymbol{R}_{1t} \\ \boldsymbol{R}_{2t} \\ \vdots \\ \boldsymbol{R}_{m,t} \end{bmatrix} \quad \boldsymbol{R}_{it} = \begin{bmatrix} \boldsymbol{R}_{it} \\ 0 \\ \vdots \\ 0 \end{bmatrix} \quad (4)$$

The diameter growth of tree k of species i and size class j from t and $t + 1$ is represented by the following model (Liang et al. 2007, 2011; notations defined in Table 1):

$$g_{ijtk} = \alpha_{i1} + \alpha_{i2}D_{tk} + \alpha_{i3}D_{tk}^2 + \alpha_{i4}B_t + \alpha_{i5}C_t + \alpha_{i6}E_t + \alpha_{i7}S_t + \alpha_{i8}H_{dt} + \alpha_{i9}H_{st} + \phi_{ijtk} \quad (5)$$

in which α_i represents parameters to be estimated with the ordinary least squares for species i based on the assumption that the prediction errors are normally distributed. Diameter growth of species i and diameter class j (g_{ijt}) is then estimated with eq. 5 in which D_{tk} is replaced by the midpoint of each diameter class D_j.

Tree mortality, $m_{ijtk} = P(M_{ijtk} = 1|x)$, is estimated with a probit model (Ai and Norton 2003) in which M_{ijtk} is a binary variable representing whether a tree of species i and diameter class j died ($M_{ijtk} = 1$) or not ($M_{ijtk} = 0$):

Table 6. Estimated parameters of the forest carbon models with diameter class.

Forest carbon models
AGL
$-3.856^{*} + 1.526B^{**} + 1.856C^{**} + 3.956E^{**} + 0.562S^{**}$
BGL
$-3.895^{**} + 0.954B^{***} + 0.682C^{*} + 2.562E^{**} + 0.896S^{*}$
AGD
$-2.856^{*} + 0.265B^{***} - 0.005C^{*} + 0.856E^{**} - 0.003S$
BGD
$-1.562^{**} + 0.856B^{***} + 0.003C + 0.267E^{**} + 0.003S$
AGLS
$3.852^{**} + 0.354B^{***} + 0.512C^{**} - 0.624E^{**} - 0.002S^{*}$
BGLS
$2.597^{**} + 0.541B^{**} + 0.621C^{**} - 0.684E^{**} - 0.005S^{*}$
AGU
$3.526^{*} - 0.031B^{***} + 0.002C^{**} + 0.084E + 0.026S^{**}$
BGU
$1.591^{**} - 0.004B^{**} + 0.001C^{*} + 0.028E + 0.004S^{**}$
Litter
$56.856^{**} + 0.526B^{**} - 0.082C^{*} + 0.851E^{**} + 0.037S^{**}$
Soil
$16.822^{***} + 0.094B^{***} + 1.561C^{***} + 2.245E^{**} + 0.037S^{**}$
SD
$3.956^{***} + 0.346B^{**} - 0.062C^{***} + 0.561E^{**} + 0.351S^{**}$
DD
$13.526^{**} + 0.526B^{***} - 0.326C^{**} - 0.526E^{**} + 0.059S^{***}$
*I*_AGB
$-4.598^{**} + 1.856B^{***} + 0.846C^{**} + 2.287E^{**} + 0.062S^{**}$
*I*_BGB
$-2.856^{**} + 0.526B^{***} + 0.521C^{***} + 0.895E^{**} + 0.267S$
*I*_Dead
$1.861^{*} + 0.856B^{***} - 0.364C^{*} + 0.095E + 0.026S^{**}$
*I*_Litter
$16.895^{**} + 0.264B^{***} + 0.056C + 0.084E^{**} + 0.062S^{**}$
*I*_Soil
$46.562^{**} + 0.856B^{***} + 0.367C^{***} + 4.589E^{**} + 0.464S^{**}$

Note: Significance levels: *, <0.05; **, <0.01; ***, <0.001.

Table 7. Estimated parameters of the forest carbon models with stand age class.

Forest carbon models
AGL
$1.526^{*} + 0.002A^{**} - 0.0002A^{2**} + 0.001N + 0.032C - 0.085E^{*} + 0.001S^{*}$
BGL
$-2.526^{**} - 0.003A^{*} + 0.0001A^{2*} + 0.002N^{*} - 0.062C + 0.034E^{*} - 0.002S^{**}$
AGD
$1.562 - 0.001A^{*} - 0.0002A^{2*} - 0.003N^{*} - 0.056C + 0.135E + 0.001S$
BGD
$1.654^{**} - 0.054A^{***} + 0.0001A^{2**} + 0.005N^{**} + 0.185C^{*} - 0.001E + 0.002S$
AGLS
$-3.851^{**} + 0.085A^{***} - 0.0002A^{2**} + 0.003N + 0.034C + 0.004E + 0.001S$
BGLS
$-0.526^{**} + 0.016A^{***} - 0.0001A^{2**} + 0.003N + 0.053C + 0.003E - 0.003S$
AGU
$2.562 - 0.152A^{***} + 0.0003A^{2***} + 0.002N^{***} + 0.186C + 0.026E + 0.002S^{*}$
BGU
$0.023 - 0.026A^{***} - 0.0001A^{2***} + 0.003N + 0.056C - 0.082E + 0.002S^{*}$
Litter
$-1.562^{*} - 0.005A^{*} - 0.0001A^{2*} - 0.004N - 0.082C + 0.264E - 0.004S^{*}$
Soil
$-0.856 + 0.001A^{*} - 0.0001A^{2*} - 0.003N - 0.059C^{*} + 0.031E - 0.002S^{*}$
SD
$-1.951^{*} - 0.084A^{***} + 0.0002A^{2**} + 0.003N^{***} + 0.086C + 0.061E + 0.001S$
DD
$-0.862^{*} - 0.062A^{**} + 0.0001A^{2***} + 0.006N^{***} + 0.001C + 0.062E + 0.011S$
*I*_AGB
$1.596 - 0.086A^{**} + 0.0002A^{2**} + 0.003N^{***} + 0.026C + 0.082E + 0.002S^{**}$
*I*_BGB
$0.852 - 0.016A^{**} + 0.0004A^{2**} + 0.001N^{***} + 0.051C - 0.033E + 0.001S^{**}$
*I*_Dead
$-1.826 + 0.063A^{*} - 0.0002A^{2*} + 0.005N^{*} - 0.056C + 0.043E + 0.003S$
*I*_Litter
$0.562^{**} - 0.026A^{*} - 0.0001A^{2*} + 0.001N - 0.053C^{*} + 0.056E^{*} - 0.001S^{**}$
*I*_Soil
$0.862 - 0.034A^{*} - 0.0005A^{2} - 0.003N + 0.051C^{*} + 0.088E + 0.002S$

Note: Significance levels: *, <0.05; **, <0.01; ***, <0.001.

$$P(M_{ijtk} = 1|x) = \Phi\left(\delta_{i1} + \delta_{i2}D_{tk} + \delta_{i3}D_{tk}^{2} + \delta_{i4}B_{t} + \delta_{i5}C_{t} + \delta_{i6}E_{t} + \delta_{i7}S_{t} + \delta_{i8}H_{dt} + \delta_{i9}H_{st} + \xi_{ijtk}\right) \quad (6)$$

where Φ is the standard normal cumulative distribution function, and δ_{is} are parameters estimated by maximum likelihood. Mortality of species i and diameter class j (m_{ijt}) is then calculated with eq. 6 in which D_{tk} is replaced by the midpoint of each diameter class D_j.

Recruitment of species i (R_i) is estimated with a Tobit model (Tobin 1958; Amemiya 1979):

$$R_{it} = \Phi\left(\beta_i x_{it}\sigma_i^{-1}\right)\beta_i x_{it} + \sigma_i\varphi\left(\beta_i x_{it}\sigma_i^{-1}\right) \quad (7)$$

with

$$\beta_i x_{it} = \beta_{i1} + \beta_{i2}N_t + \beta_{i3}N_t^{2} + \beta_{i4}B_t + \beta_{i5}C_t + \beta_{i6}E_t + \beta_{i7}S_t + \beta_{i8}H_{dt} + \beta_{i9}H_{st} + \mu_{it} \quad (8)$$

where Φ is the standard normal cumulative distribution function and φ is the standard normal probability density function. The Tobit model explicitly accounts for unobserved recruitment values that are left-censored at the preset diameter limit (2.54 cm).

The C stock of pool i from t and $t + 1$ was estimated from stand basal area with the following model:

$$\psi_{it} = \omega_{i1} + \omega_{i2}B_t + \omega_{i3}C_t + \omega_{i4}E_t + \omega_{i5}S_t + \omega_{i6}H_{dt} + \omega_{i7}H_{st} + \varepsilon_{it} \quad (9)$$

in which ψ_{it} is the C of pool i at time t, ω_i are parameters to be estimated with the ordinary least squares for pool i, and ψ_{it} is calculated with eq. 9.

No replacement disturbances were considered for the short-term prediction (5-year period between two inventories) as the plot re-measurement period of FIA in the eastern US is between 5 and 7 years.

Matrix model structure for stand age class

$\mathbf{Z}_t$ and $\mathbf{Z}_{it}$ are matrices used to model forest C dynamics, where

$$\mathbf{Z}_t = \begin{bmatrix} \mathbf{Z}_{1t} & & & \\ & \mathbf{Z}_{2t} & & \\ & & \ddots & \\ & & & \mathbf{Z}_{i,t} \end{bmatrix}$$

$$\mathbf{Z}_{it} = \begin{bmatrix} e_{1,t} & & & & \\ f_{1,t} & e_{2,t} & & & \\ & \ddots & \ddots & & \\ & & f_{i-2,t} & e_{i-1,t} & \\ & & & f_{i-1,t} & e_{i,t} \end{bmatrix} \quad (10)$$

in which e_{it} represents the probability that C of stand age class i stays in the same stand age class between t and $t + 1$; and f_{it}, the

Fig. 2. Mean predicted and observed basal areas at the second inventory for the matrix growth model with tree diameter class, including the 95% confidence interval of the observed mean, for common forest types in the Northern Forest region (Maine, New Hampshire, New York, and Vermont, US).

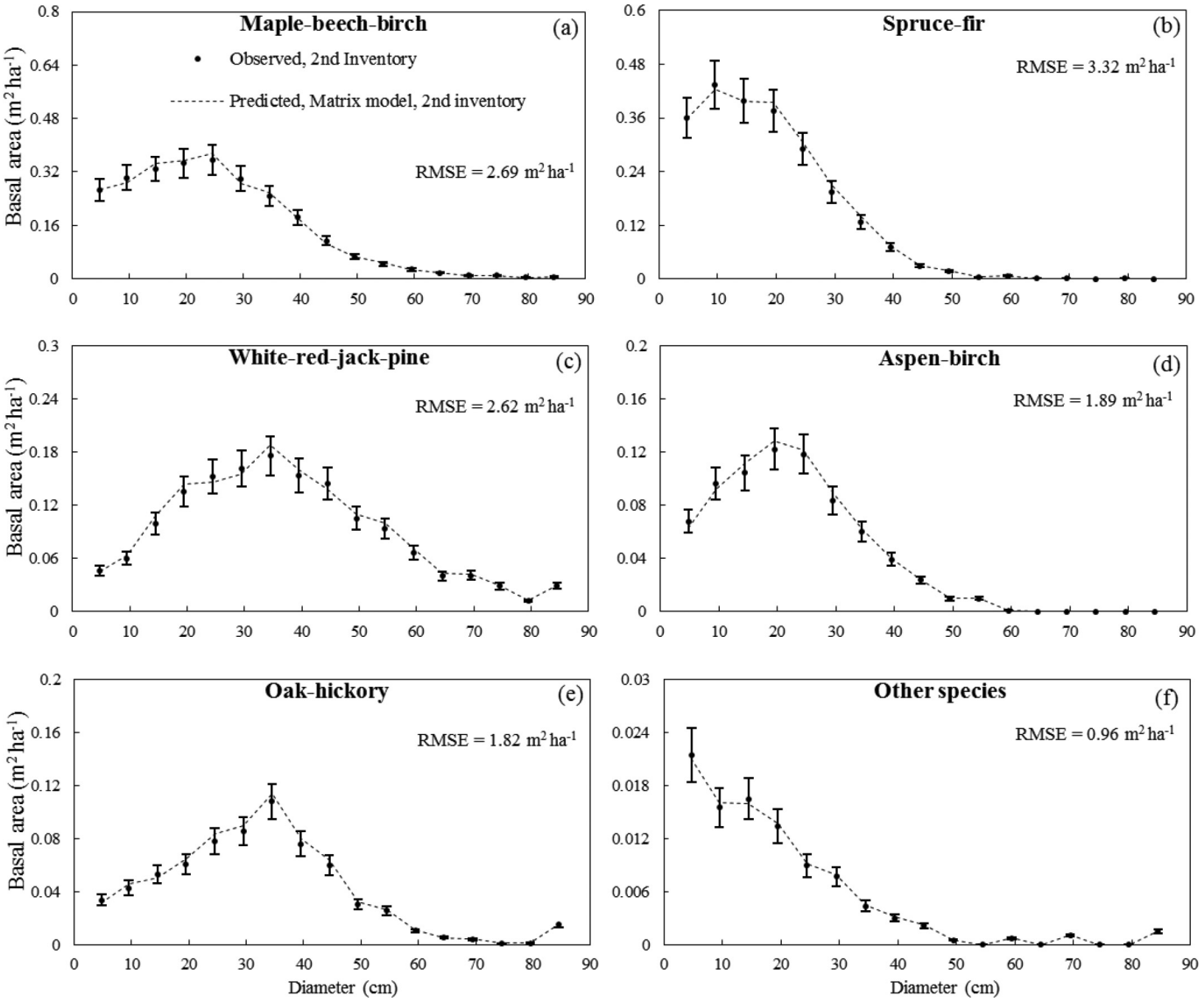

probability of C move, is estimated as the forest C move f_{it} between t and $t + 1$.

The C move of stand age class i from t and $t + 1$ is represented by the following model:

$$\gamma_{it} = \theta_{i1} + \theta_{i2}A_t + \theta_{i3}A_t^2 + \theta_{i4}N_t + \theta_{i5}C_t + \theta_{i6}E + \theta_{i7}S_t + \delta_{it} \quad (11)$$

in which θ_i are parameters to be estimated with the ordinary least squares for stand age class i; γ_{it} is then calculated with eq. 11 in which A_t is replaced by the midpoint of each stand age class A_i.

No recruitment, mortality, and replacement disturbances were considered for the short-term prediction (5-year period between two inventories) in a manner similar to the diameter class matrix model. All analyses were conducted with the R program (version R 3.3.3, R Foundation for Statistical Computing, Vienna, Austria; http://www.R-project.org/) using packages survival, AER, lmtest, and rms.

Both structural diversity (H_s) and species diversity (H_d) are calculated with Shannon's model (Pielou 1977):

$$H_s = -\sum_{i=1}^{m} \frac{B_i}{B} \ln\left(\frac{B_i}{B}\right), \qquad H_d = -\sum_{j=1}^{n} \frac{B_j}{B} \ln\left(\frac{B_j}{B}\right) \quad (12)$$

where B_i, B_j, and B are the basal area of species group i, size class j, and total basal area, respectively.

Fuzzy sets representing uncertainty

Uncertainty analysis is a necessary and important component in model simulation (Ma and Zhou 2018). Uncertainty leads to high variability in predicted values of forest C stock. Here we used fuzzy sets that involved defining membership functions that determined the level of uncertainty (Zadeh 1965). Fuzzy set approaches permit the gradual assessment of the membership of elements in a set; this is described with the aid of a membership function valued in the real unit interval [0, 1] (Zadeh 1965). A trap-

Fig. 3. Mean predicted and observed values for the 12 carbon pools and five IPCC carbon pools at the second inventory for the matrix growth model with tree diameter class and stand age class, including the 95% confidence interval of the observed mean. An asterisk (*) after "AGL" and "Soil" indicates that their real values should be multiplied by 10 as they are too large to show in the same figure with the other carbon pools. D, diameter class; S, stand age class). [Colour version online.]

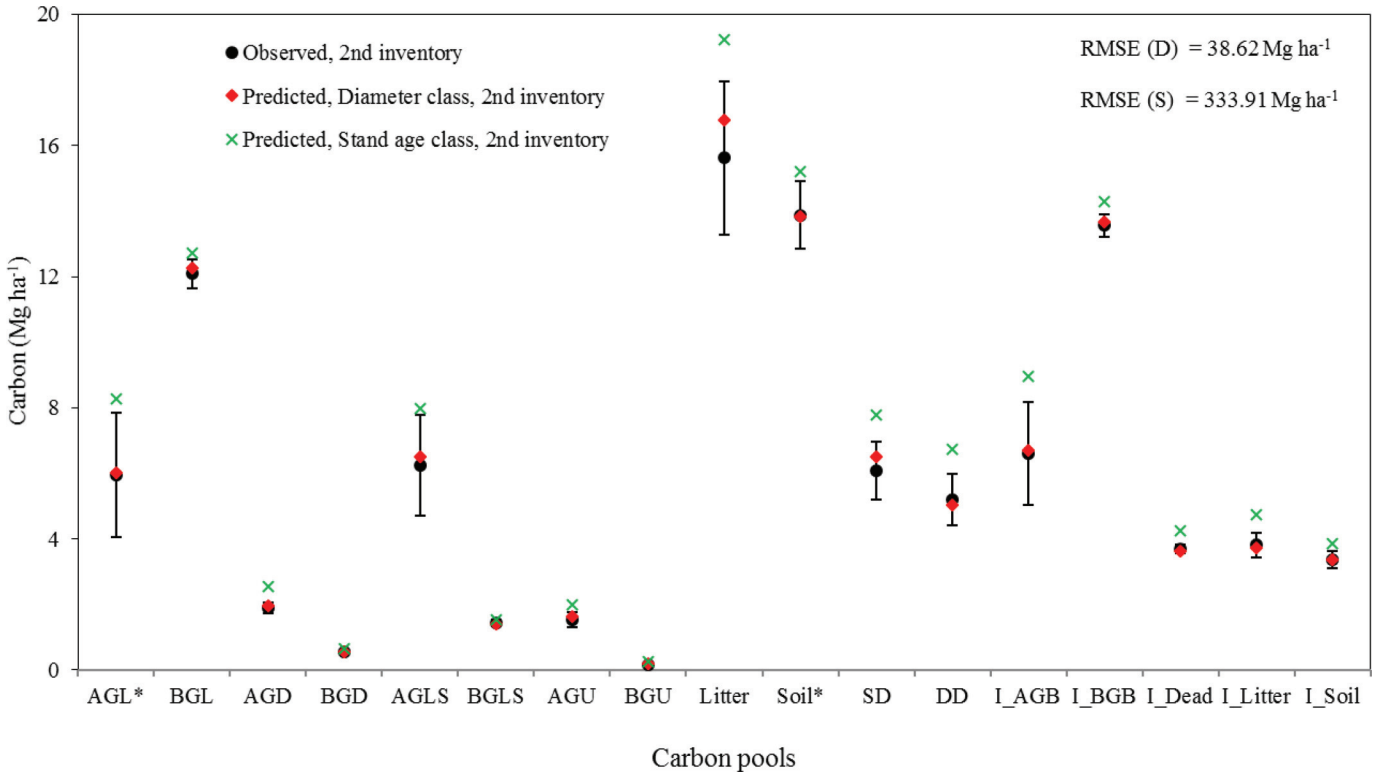

ezoidal fuzzy set was used, mathematically expressed as $f(x; a, b, c, d) = \max(\min(x - ab - a, 1, d - xd - c), 0)$ in which $[b, c]$ represents the certainty interval for which the membership degree is 1, $[a, b]$ and $[c, d]$ are the uncertainty intervals with membership degrees ranging from 0 to 1, and $[a, d]$ is a measure of total range of uncertainty. Following Weckenmann and Schwan (2001), given the mean value of predicted C ($\overline{X}$) and its relative standard deviation (S_r) from simulations, a, b, c, and d values can be calculated as follows:

$$
\begin{aligned}
b &= \frac{\overline{X}}{1 + 0.5S_r} \\
c &= \overline{X}(1 + 0.5S_r) \\
a &= b - \overline{X}\left(\frac{1}{1 + 0.5S_r} - \frac{1}{1 + 2.5S_r}\right) \\
d &= c + \overline{X} \cdot 2S_r
\end{aligned}
\tag{13}
$$

Results

Summary statistics of plot and tree variables

Among the plot-level variables studied, the mean recruitment (R) and stem density (N) were highest for spruce–fir and lowest for other species categories (Supplementary Table S3[1]). The mean interval between two inventories was 5 years. In the 12 C pools of the current measurement, soil C had the highest density (138.76 Mg·ha^{-1}) and the highest increase from the previous measurement (10.42 Mg·ha^{-1}), and belowground understory had the lowest C density (0.17 Mg·ha^{-1}) and the lowest increase from the previous measurement (0.02 Mg·ha^{-1}). In the five IPCC C pools of the current measurement, aboveground C had the highest value (63.31 Mg·ha^{-1}) and the highest increase (2.77 Mg·ha^{-1}), while deadwood C had the smallest value (3.69 Mg·ha^{-1}) and lowest increase (0.08 Mg·ha^{-1}) (Tables 1 and 2). At the individual-tree level, the white–red–jack pine species group had the largest diameter at breast height (D) and annual diameter growth (g) and the lowest mortality rate (m). Spruce–fir had the smallest diameter at breast height (D), while aspen–birch had the highest mortality rate (m) (Supplementary Table S4[1]).

Parameters of C flux matrix models

The dependent variables, i.e., the mean annual rates of growth, mortality, recruitment, and the 12 C pools and five IPCC C pools, were estimated from tree and stand attributes using repeated measurements of 5178 permanent ground plots (Tables 3–7). The explanatory variables were selected based on statistical and biological significance. The primary control variables for the matrix models (diameter at breast height (D), stand basal area (B), stem density (N), and stand age (A)) were all significant at the $\alpha \leq 0.05$ level (Tables 3–7). Mortality rate declined significantly with stand basal area. The recruitment of a species increased strongly with the density of that species in the stand. Tree abundance was the most significant predictor of recruitment and its effect was consistent across all species groups. In most C pools, greater stand basal area and stand density may have more C density, while higher stand age may produce less C density over time.

Predictions of forest C

For the 1294 validation plots, the basal area by species and diameter class predicted by the matrix models fell within the 95% confidence interval of the observed values in all 51 species diameter classes, demonstrating accuracy of the matrix models. Therefore, predicted stand conditions were well aligned with the mean estimates (Fig. 2). In addition, the predictions for the 12 C pools and five IPCC C pools all fell within the 95% confidence interval of the estimated means (Fig. 3). Based on the root mean square error (RMSE), the matrix models with diameter class had short-term accuracy as well (Fig. 3). Compared with diameter class, the C

Fig. 4. Mean predicted and observed values for four carbon pools and four IPCC carbon pools at the second inventory for the matrix growth model with stand age class, including the 95% confidence interval of the observed mean. Note that the rest of the carbon pools are displayed in the Supplementary material[1].

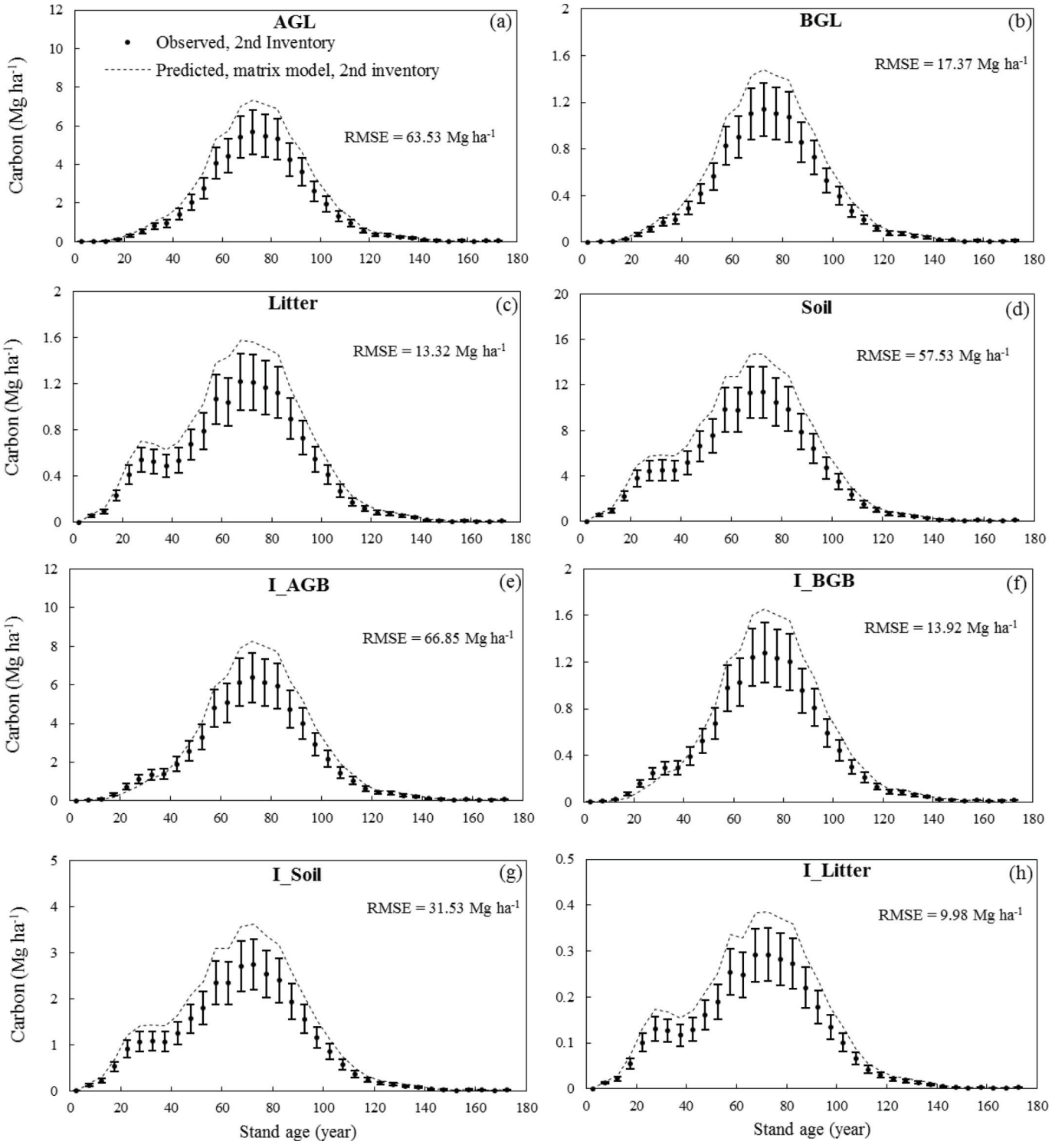

pools by stand age class predicted by the matrix model fell outside the 95% confidence interval of the observed values, demonstrating a low accuracy (Fig. 4; Supplementary Fig. S1[1]). Based on the significantly higher RMSE than the diameter class, the matrix models with stand age class displayed poor short-term accuracy as well (Fig. 4; Supplementary Fig. S1[1]). Based on the 30-year prediction, mean predicted aboveground C and soil C by diameter class increased over time and converged to ~89 Mg·ha^{-1} and ~168 Mg·ha^{-1}, respectively, by 2045. In comparison, mean predicted aboveground C and soil C by stand age class had a much higher increase over time, converging to around 117 Mg·ha^{-1} and 196 Mg·ha^{-1}, respectively, at the end of 2045 (Fig. 5).

Fig. 5. Mean predicted (*a*) aboveground carbon and (*b*) soil carbon for the matrix growth model with tree diameter class and stand age class.

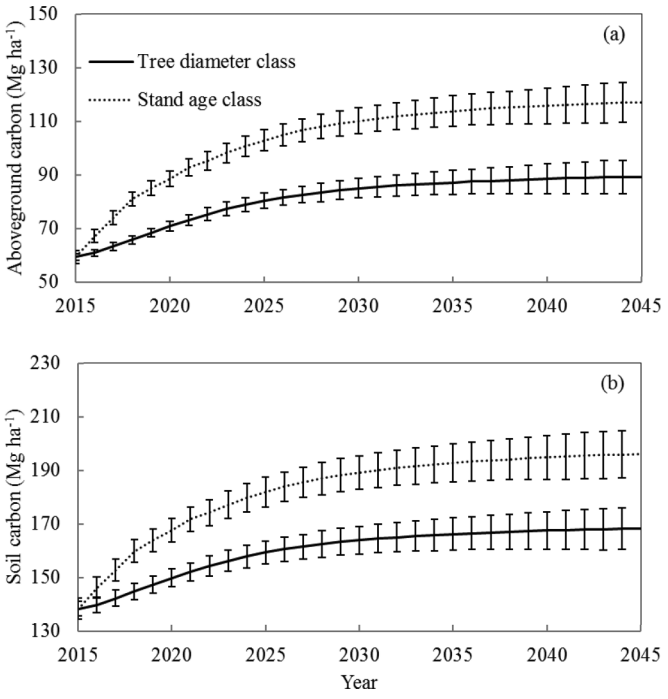

Uncertainty analysis

To account for variability and sources of imprecision in the simulation results, fuzzy sets were constructed for tree diameter class and stand age class based on model 13. Stand age class could lead to higher estimates of aboveground C and soil C than tree diameter class. There were no overlaps between fuzzy sets of tree diameter class and stand age class (Fig. 6), indicating that predictions of aboveground C and soil C would be distinctively different in tree diameter class and stand age class with high certainty.

Discussion

Comparison of size-structured models with age-structured models in their capacity to estimate forest C dynamics is crucial for improving projections of current forest C baselines to meet international and domestic greenhouse gas reporting requirements. In this study, we applied C flux matrix models by tree diameter class and stand age class to predict forest C dynamics over a short-term period. In the C flux matrix models by diameter class, C density was found to be positively correlated with stand basal area for most C pools. Site productivity, elevation, and slope, which jointly affected forest C productivity, soil temperature and moisture, evapotranspiration rate, and radiation (Stage and Salas 2007; Liang and Zhou 2014), may have positive effects on the sequestration status of most C pools in the study. In the C flux matrix models by stand age class, negative relations between C density and stand age were found over most of the C pools, whereas positive relationships were found between C density and stand density. This finding suggests that younger and denser stands would have higher sequestration rates than older and (or) poorly stocked stands; however, the age data, particularly for older stands, should be interpreted with caution given the methodological challenges associated with accurately assessing age in older forest stands. In addition, site productivity, elevation, and slope did not significantly affect the status of most C pools.

In past studies, Usher (1966, 1969) developed size-structured models in replacement of age-structured models for uneven forest stands as the age-structured models did not provide accurate results as expected. Forest C prediction with diameter or stand age classes was made to improve the characterization of forest C dynamics (Liang and Zhou 2014; Ma and Zhou 2018) but with little examination of the accuracy of forest C prediction by diameter versus stand age in a quantitative calculation. Stand age, which is related to time and is a predicable attribute over time, is a useful surrogate variable for analyses of forest C dynamics (Pan et al. 2011*b*). Previous studies focused on the estimation of C flux by stand age class (Yarie and Parton 2005; Pan et al. 2011*b*), estimated from limited and unrepresentative forest inventory data and subject to uncertainty caused by age data. Another issue is that of uneven-aged stands that contain a variety of small, medium, and large trees (Tyrrell and Crow 1994) whereby the use of stand age will be of little use in estimating C dynamics. In comparison, the use of diameter classes can reasonably represent the diverse structures of uneven-aged stands, an approach demonstrated in this study with the diameter predictor providing a convenient framework for analyzing systematic variation in forest C across a wide range of structural stages. Through considering the combined effects of variability in tree growth, recruitment, and mortality rates, the C flux matrix models with diameter class may enable better predictions of forest population dynamics associated with forest C dynamics than stand age class. Comparing the C simulation results and RMSE of C flux matrix models by tree diameter class and stand age class, we found that diameter had a significantly more accurate estimate of C stock status than stand age. This finding was consistent with previous research that examined diameter as a superior metric relative to stand age in terms of describing structural development for uneven-aged northern hardwood forests over time (Lorimer and Frelich 1997). We also found that mean predicted aboveground C and soil C by stand age class had a much higher increase over time than diameter class by 2045. This result indicates that the stand age predictor may overestimate the aboveground C and soil C over 30 years without considering natural disturbances and land-use change.

Our estimates of plot-level C used empirical C flux matrix models to estimate each C pool with inputs from repeated measures of tree- and plot-level variables. These models of C stocks by C pool are the basis for estimating forest land C in U.S. National Greenhouse Gas Inventories and represent best approximations for each pool (U.S. Environmental Protection Agency (EPA) 2017). They enabled explicit prediction of C sequestration or emissions by species and diameter or age. In this study, we found that diameter aligns better with biometrical modelling and other stand attributes such as basal area, volume, biomass, growth rate, mortality, and regeneration (Liang 2012; Peterson et al. 2014; Liang and Zhou 2014; Ma et al. 2016; Ma and Zhou 2018). In addition to higher accuracy, diameter data are also much easier to acquire from forest inventories and can represent a diversity of stand structures across a collection of diverse tree species.

In our study, we only examined the total basal area as an absolute measure of stand density and indicator of competition in the individual-tree models. Moreover, the use of basal area of trees larger than a given target tree and relative density have been used in many other models as an additional predictor of competition (e.g., Wycoff 1990); however, this approach was not used in this study. Hence, the model presented here can be improved in the future through incorporation of additional competitive factors. On the other hand, empirical models such as the ones used in this study have inherent caveats. For example, they are highly sensitive to the sample plots used for calibration and do not describe ecological processes associated with tree growth, regeneration, and C dynamics. Hence, these models configured for C estimation and reporting initiatives have limited ability in making ecological inferences. Extrapolating predictions made by these models to longer time periods or regions larger than the one represented by the data warrants caution; therefore, its long-term simulations were subject to uncertainty caused by extrapolating predictions.

Fig. 6. Fuzzy sets representing uncertainty in the (*a*) aboveground carbon and (*b*) soil carbon for the tree diameter class and stand age class from 2015 to 2045.

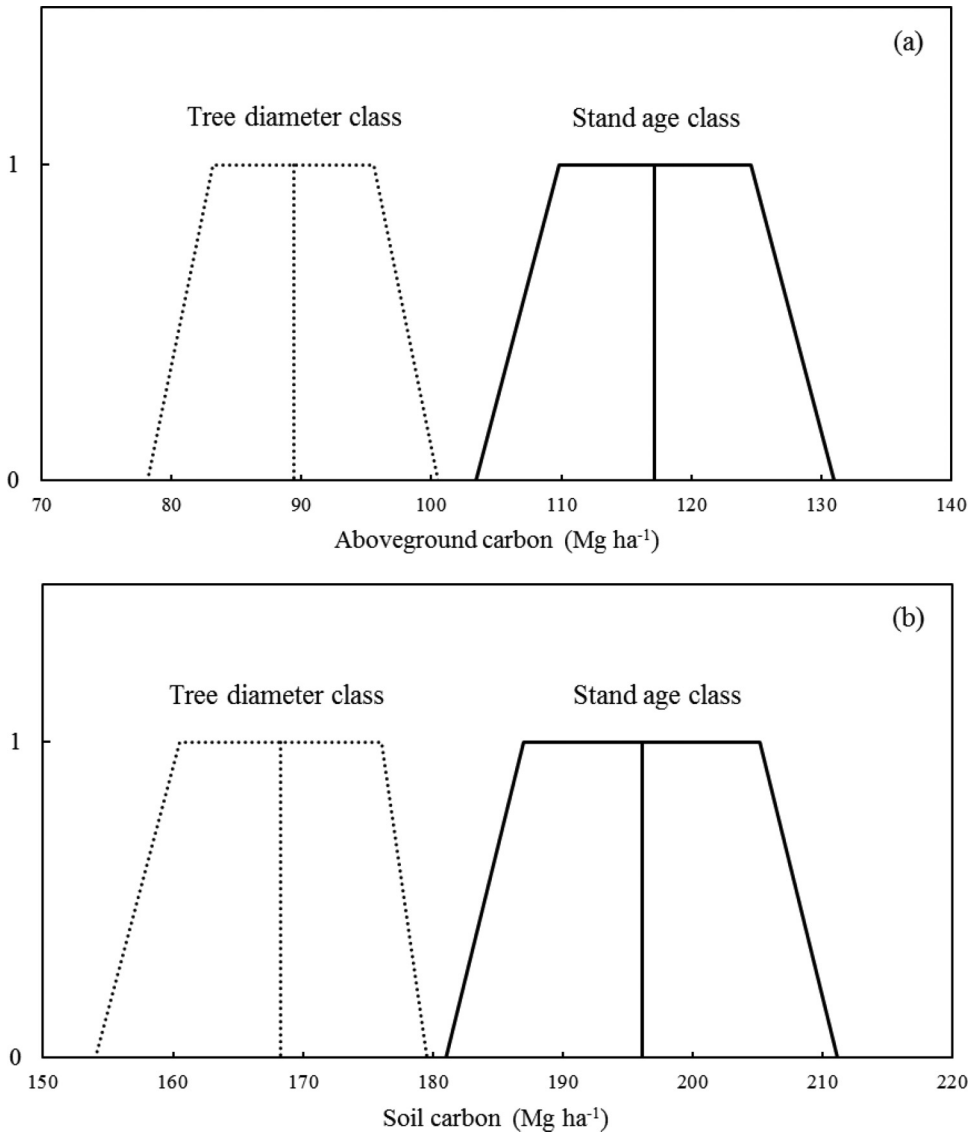

Additionally, a challenge for fitting the transition probabilities in the matrix model can arise when empirical observations of stand conditions over time indicate that stand age or diameter class progress at a rate beyond the constraints of the matrix model (Rogers-Bennett and Rogers 2006; Liang and Picard 2013). Such a situation can arise when stands move forward or backward by more than one class.

Beyond stand dynamics, the spatial scale and regional land-use matrix present forest C simulation hurdles. The C flux matrix models were less precise as the distance of study region from the sampled area increased (Liang et al. 2011). In addition, they did not reflect land-use change (from non-forest to forest or from forest to non-forest) and major natural disturbances such as climate change, wildfires, insects, hurricanes, and widespread diseases. We used fuzzy sets to examine the possible ranges in predictions of aboveground C and soil C as an index of uncertainty, while explicitly examining individual sources of uncertainty was not considered in the study. As such, caution should be extended to applying this study's models in the context of individual drivers of C flux.

A primary motivation for developing the C flux matrix model in this study was to generate a useful baseline tool for the estimation of future C dynamics with the most up-to-date estimates (i.e., incorporation of recent annual inventory data) across the entire reporting period from 1990 to the present in future research. The effects of land-use change and natural disturbances could be addressed by incorporating the present model with a transition matrix of land-use change and stochastic elements of disturbances (Zhou and Buongiorno 2006; Woodall et al. 2015; Wear and Coulston 2015). The C flux matrix models would align with the land-use change matrix (tracking stocks of C across discrete classes over time) and more accurately characterize the effects of land-use change on forest C stock with diameter class. Land-use change involves transfers between forests and other land uses (e.g., urban, farm, and industrial establishments). Estimates of area transitioning from a non-forest use to a forest use can be used as an increase matrix in the forest C flux matrix while transition from forest to non-forest use can be adopted as a loss matrix from the forest C flux matrix. Therefore, the developed C flux matrix models could be viewed as the first step toward more robust fu-

ture evaluations of the C dynamics associated with land-use change. More importantly, the matrix growth model also could be useful for providing spatially and temporally explicit forest C dynamics at large scales by incorporating predictions of vegetation indices from Landsat data to pixels (i.e., population units) with a geospatial matrix over long-term periods (Liang and Zhou 2014).

Applying the matrix models to study forest C dynamics outside the sample area is admittedly a difficult task, as model extrapolation often causes greater uncertainty. The question is whether the model would have the same accuracy with a set of plots that have the same range of values for the predictors considered in the model but different values for other environmental variables not considered as predictors in the model. Nonrandom cross-validation may be useful in this context (see, e.g., Wenger and Olden 2012). To this end, the accuracy and precision of current forest C dynamics could be further improved by including additional variables such as predictions of vegetation indices from remotely sensed data that are temporally consistent and spatially continuous facilitating estimation over large or small spatial scales.

Conclusion

The simulation of forest C dynamics over relatively short time frames (e.g., 5–30 years) is necessary to meet both international reporting requirements (e.g., UNFCCC) and atmospheric CO_2 mitigation targets (e.g., Paris COP; Morgan 2016). Despite this, tremendous uncertainty exists for all nations in their efforts to track forest land C trends across time, diverse forest C pools, large spatial extents, and varying land uses and disturbance dynamics. Although we found that C flux matrix models based on tree diameter classes were far superior to those based on stand age classes in terms of predicting forest C dynamics over short-term periods, large knowledge gaps and research opportunities remain. The effect of forest C model selection on resulting forest C baseline projections and policy implications is evident given that we found that mean predicted aboveground C and soil C by stand age class were much higher than when using diameter class by 2045. As our study found that tree diameter was a much better predictor of forest C changes than stand age over our study's time period, the opportunity exists to more deeply explore improvements of forest C baseline monitoring procedures (e.g., incorporation of spatially and temporal explicit and (or) reduced-latency data) to the betterment of regional, national, and international estimation and reporting initiatives.

Acknowledgements

This study is supported by the USDA Forest Service Northern Research Station and the Department of Interior Northeast Climate Science Center. We thank the USDA Forest Service for providing FIA data. The Associate Editors and three anonymous reviews provided comments that improved a previous version of this paper.

References

Ai, C., and Norton, E.C. 2003. Interaction terms in logit and probit models. Econ. Lett. **80**: 123–129. doi:10.1016/S0165-1765(03)00032-6.

Amemiya, T. 1979. The estimation of a simultaneous-equation Tobit model. Int. Econ. Rev. **20**: 169–181. doi:10.2307/2526423.

Boltz, F., and Carter, D.R. 2006. Multinomial logit estimation of a matrix growth model for tropical dry forests of eastern Bolivia. Can. J. For. Res. **36**(10): 2623–2632. doi:10.1139/x06-155.

Caswell, H. 2001. Matrix population models. John Wiley & Sons.

Evans, A.M., and Perschel, R. 2009. A review of forestry mitigation and adaptation strategies in the Northeast US. Climatic Change, **96**(1–2): 167–183.

Felfili, J.M. 1995. Growth, recruitment and mortality in the Gama gallery forest in central Brazil over a six-year period (1985–1991). J. Trop. Ecol. **11**: 67–83. doi:10.1017/S0266467400008415.

Fieberg, J., and Ellner, S.P. 2001. Stochastic matrix models for conservation and management: a comparative review of methods. Ecol. Lett. **4**: 244–266. doi:10.1046/j.1461-0248.2001.00202.x.

Gove, J.H., and Ducey, M.J. 2014. Optimal uneven-aged stocking guides: an application to spruce–fir stands in New England. Forestry, **87**: 61–70. doi:10.1093/forestry/cpt040.

Gunn, J.S., Ducey, M.J., and Whitman, A.A. 2014. Late-successional and old-growth forest carbon temporal dynamics in the Northern Forest (Northeastern USA). For. Ecol. Manage. **312**: 40–46. doi:10.1016/j.foreco.2013.10.023.

Huth, A., and Ditzer, T. 2001. Long-term impacts of logging in a tropical rain forest — a simulation study. For. Ecol. Manage. **142**: 33–51. doi:10.1016/S0378-1127(00)00338-8.

Intergovernmental Panel on Climate Change (IPCC). 2006. Guidelines for National Greenhouse Gas Inventories. Volume 4: Agriculture, Forestry and Other Land Use. *Prepared by* the National Greenhouse Gas Inventories Programme. *Edited by* H.S. Eggleston, L. Buendia, K. Miwa, T. Ngara, and K. Tanabe. IGES, Japan.

Lennon, J.J., Kunin, W.E., Corne, S., Carver, S., and van Hees, W.W.S. 2002. Are Alaskan trees found in locally more favourable sites in marginal areas? Global Ecol. Biogeogr. **11**: 103–114. doi:10.1046/j.1466-822X.2002.00279.x.

Leslie, P.H. 1945. On the use of matrices in certain population mathematics. Biometrika, **33**: 183–212. doi:10.1093/biomet/33.3.183. PMID:21006835.

Lewis, E.G. 1977. On the generation and growth of a population. *In* Mathematical demography. *Edited by* D.P. Smith and N. Keyfitz. Springer, Berlin, Heidelberg. pp. 221–225. doi:10.1007/978-3-642-81046-6_25.

Liang, J. 2012. Mapping large-scale forest dynamics: a geospatial approach. Landscape Ecol. **27**: 1091–1108. doi:10.1007/s10980-012-9767-7.

Liang, J., and Picard, N. 2013. Matrix model of forest dynamics: an overview and outlook. For. Sci. **59**: 359–378. doi:10.5849/forsci.11-123.

Liang, J., and Zhou, M. 2014. Large-scale geospatial mapping of forest carbon dynamics. J. Sustainable For. **33**: S104–S122. doi:10.1080/10549811.2014.883998.

Liang, J., Buongiorno, J., Monserud, R.A., Kruger, E.L., and Zhou, M. 2007. Effects of diversity of tree species and size on forest basal area growth, recruitment, and mortality. For. Ecol. Manage. **243**: 116–127. doi:10.1016/j.foreco.2007.02.028.

Liang, J., Zhou, M., Verbyla, D.L., Zhang, L., Springsteen, A.L., and Malone, T. 2011. Mapping forest dynamics under climate change: a matrix model. For. Ecol. Manage. **262**: 2250–2262. doi:10.1016/j.foreco.2011.08.017.

Lorimer, C.G., and Frelich, L.E. 1997. A structural alternative to chronosequence analysis for uneven-aged northern hardwood forests. J. Sustainable For. **6**: 347–366. doi:10.1300/J091v06n03_07.

Loudermilk, E.L., Scheller, R.M., Weisberg, P.J., Yang, J., Dilts, T.E., Karam, S.L., and Skinner, C. 2013. Carbon dynamics in the future forest: the importance of long-term successional legacy and climate–fire interactions. Global Change Biol. **19**: 3502–3515. doi:10.1111/gcb.12310.

Ma, W., and Zhou, M. 2018. Assessments of harvesting regimes in central hardwood forests under climate and fire uncertainty. For. Sci. **64**: 57–73.

Ma, W., Liang, J., Cumming, J.R., Lee, E., Welsh, A.B., Watson, J.V., and Zhou, M. 2016. Fundamental shifts of central hardwood forests under climate change. Ecol. Modell. **332**: 28–41. doi:10.1016/j.ecolmodel.2016.03.021.

MacLean, R.G., Ducey, M.J., and Hoover, C.M. 2014. A comparison of carbon stock estimates and projections for the northeastern United States. For. Sci. **60**: 206–213. doi:10.5849/forsci.12-072.

Morgan, J. 2016. Paris COP 21: power that speaks the truth? Globalizations, **13**: 943–951. doi:10.1080/14747731.2016.1163863.

Namaalwa, J., Eid, T., and Sankhayan, P. 2005. A multi-species density-dependent matrix growth model for the dry woodlands of Uganda. For. Ecol. Manage. **213**: 312–327. doi:10.1016/j.foreco.2005.03.024.

Pan, Y., Birdsey, R.A., Fang, J., Houghton, R., Kauppi, P.E., Kurz, W.A., Phillips, O.L., Shvidenko, A., Lewis, S.L., Canadell, J.G., Ciais, P., Jackson, R.B., Pacala, S.W., McGuire, A.D., Piao, S., Rautiainen, A., Sitch, S., and Hayes, D. 2011*a*. A large and persistent carbon sink in the world's forests. Science, **333**: 988–993. doi:10.1126/science.1201609. PMID:21764754.

Pan, Y., Chen, J.M., Birdsey, R., McCullough, K., He, L., and Deng, F. 2011*b*. Age structure and disturbance legacy of North American forests. Biogeosciences, **8**: 715–732. doi:10.5194/bg-8-715-2011.

Peterson, R.L., Liang, J., and Barrett, T.M. 2014. Modeling population dynamics and woody biomass in Alaska coastal forest. For. Sci. **60**: 391–401. doi:10.5849/forsci.12-540.

Pielou, E. 1977. Mathematical ecology. John Wiley & Sons, New York.

Rhemtulla, J.M., Mladenoff, D.J., and Clayton, M.K. 2009. Historical forest baselines reveal potential for continued carbon sequestration. Proc. Natl. Acad. Sci. **106**: 6082–6087. doi:10.1073/pnas.0810076106. PMID:19369213.

Rice, A.H., Pyle, E.H., Saleska, S.R., Hutyra, L., Palace, M., Keller, M., de Camargo, P.B., Portilho, K., Marques, D.F., and Wofsy, S.C. 2004. Carbon balance and vegetation dynamics in an old-growth Amazonian forest. Ecol. Appl. **14**: 55–71. doi:10.1890/02-6006.

Rogers-Bennett, L., and Rogers, D.W. 2006. A semi-empirical growth estimation method for matrix models of endangered species. Ecol. Modell. **195**: 237–246. doi:10.1016/j.ecolmodel.2005.11.019.

Solomon, D.S., Hosmer, R.A., and Hayslett, H.T. 1987. FIBER handbook: a growth model for spruce–fir and northern hardwood types. USDA Forest Service, Northeastern Forest Experiment Station, Broomall, Pennsylvania, Res. Pap. NE-RP-602.

Solomon, D.S., Herman, D.A., and Leak, W.B. 1995. FIBER 3.0: an ecological growth model for northeastern forest types. USDA Forest Service, Northeastern Forest Experiment Station, Radnor, Pennsylvania, Gen. Tech. Rep. NE-204.

Solomon, D.S., Brann, T.B., and Caldwell, L.E. 2000. Adaptation of FIBER for forest inventory and analysis growth projections in the state of Maine. *In* Integrated tools for natural resources inventories in the 21st century. *Edited by* M. Hansen and T. Burk. USDA Forest Service, North Central Forest Experiment Station, St. Paul, Minnesota, Gen. Tech. Rep. NC-212. pp. 580–586.

Stage, A.R., and Salas, C. 2007. Interactions of elevation, aspect, and slope in models of forest species composition and productivity. For. Sci. **53**: 486–492.

Swaine, M.D., Lieberman, D., and Putz, F.E. 1987. The dynamics of tree populations in tropical forest: a review. J. Trop. Ecol. **3**: 359–366. doi:10.1017/S0266467400002339.

Tobin, J. 1958. Estimation of relationships for limited dependent variables. Econometrica, **26**: 24–36. doi:10.2307/1907382.

Tyrrell, L.E., and Crow, T.R. 1994. Structural characteristics of old-growth hemlock–hardwood forests in relation to age. Ecology, **75**: 370–386. doi:10.2307/1939541.

U.S. Department of Agriculture Forest Service. 2014. Forest Inventory and Analysis Database (FIADB) version 5.1 [online]. Available from https://apps.fs.usda.gov/fia/datamart/datamart.html [accessed 1 August 2018].

U.S. Department of Agriculture Forest Service. 2015. The Forest Inventory and Analysis Database: database description and user guide for Phase 2 (version 6.0.2). Available from https://www.fia.fs.fed.us/library/database-documentation/current/ver72/FIADB%20User%20Guide%20P2_7-2_final.pdf [accessed 1 August 2018].

U.S. Environmental Protection Agency (EPA). 2017. Inventory of U.S. greenhouse gas emissions and sinks (1990–2015). U.S. Environmental Protection Agency, Washington, D.C.

Usher, M.B. 1966. A matrix approach to the management of renewable resources, with special reference to selection forests. J. Appl. Ecol. **3**: 355–367. doi:10.2307/2401258.

Usher, M.B. 1969. A matrix model for forest management. Biometrics, **25**: 309–315. doi:10.2307/2528791.

Vieira, S., de Camargo, P.B., Selhorst, D., da Silva, R., Hutyra, L., Chambers, J.Q., Brown, I.F., Higuchi, N., dos Santos, J., Wofsy, S.C., and Trumbore, S.E. 2004. Forest structure and carbon dynamics in Amazonian tropical rain forests. Oecologia, **140**: 468–479. doi:10.1007/s00442-004-1598-z. PMID:15221436.

Wear, D.N., and Coulston, J.W. 2015. From sink to source: regional variation in U.S. forest carbon futures. Sci. Rep. **5**: 16518. doi:10.1038/srep16518. PMID:26558439.

Weckenmann, A., and Schwan, A. 2001. Environmental life cycle assessment with support of fuzzy-sets. Int. J. LCA, **6**: 13–18. doi:10.1007/BF02977589.

Wenger, S.J., and Olden, J.D. 2012. Assessing transferability of ecological models: an underappreciated aspect of statistical validation. Methods Ecol. Evol. **3**: 260–267. doi:10.1111/j.2041-210X.2011.00170.x.

Woodall, C.W., Walters, B.F., Coulston, J.W., D'Amato, A.W., Domke, G.M., Russell, M.B., and Sowers, P.A. 2015. Monitoring network confirms land use change is a substantial component of the forest carbon sink in the eastern United States. Sci. Rep. **5**: 17028. doi:10.1038/srep17028. PMID:26639409.

Wycoff, W.R. 1990. A basal area increment model for individual conifers in the northern Rocky Mountains. For. Sci. **36**: 1077–1104.

Yarie, J., and Parton, B. 2005. Potential changes in carbon dynamics due to climate change measured in the past two decades. Can. J. For. Res. **35**(9): 2258–2267. doi:10.1139/x05-106.

Zadeh, L.A. 1965. Fuzzy sets. Inf. Control, **8**: 338–353. doi:10.1016/S0019-9958(65)90241-X.

Zhou, M., and Buongiorno, J. 2006. Forest landscape management in a stochastic environment, with an application to mixed loblolly pine–hardwood forests. For. Ecol. Manage. **223**: 170–182. doi:10.1016/j.foreco.2005.10.068.